

# Uncertainty estimation for out-of-distribution detection in computational histopathology

Lea Goetz

Artificial Intelligence and Machine Learning, GSK, London  
lea.x.goetz@gsk.com

## Abstract

In computational histopathology algorithms now outperform humans on a range of tasks, but to date none are employed for automated diagnoses in the clinic. Before algorithms can be involved in such high-stakes decisions they need to "know when they don't know", i.e., they need to estimate their predictive uncertainty. This allows them to defer potentially erroneous predictions to a human pathologist, thus increasing their safety. Here, we evaluate the predictive performance and calibration of several uncertainty estimation methods on clinical histopathology data. We show that a distance-aware uncertainty estimation method outperforms commonly used approaches, such as Monte Carlo dropout and deep ensembles. However, we observe a drop in predictive performance and calibration on novel samples across all uncertainty estimation methods tested. We also investigate the use of uncertainty thresholding to reject out-of-distribution samples for selective prediction. We demonstrate the limitations of this approach and suggest areas for future research.

## 1 Introduction

Over the last decade, computational histopathology has seen a surge in algorithms achieving equal or superior performance compared to human pathologists on a diverse set of tasks, such as metastasis detection [Liu et al., 2019], prediction of molecular markers from tissues [Naik et al., 2020], and patient survival [Mobadersany et al., 2018]. However, despite these academic successes, none of these models have to date been used in a decision making capacity in a clinical setting, and only one software is approved for assisting pathologists<sup>1</sup>. What explains this *translation gap*? In addition to model-independent hurdles (e.g., regulatory approval, integration into clinical workflows, etc. [Steiner et al., 2021]), a key requirement for models in high-stakes applications is robustness to data shift. However, in histopathology datasets are generally small (compared to standard ML datasets, such as ImageNet) and models trained on them are more likely to overfit low-level features [Arpit et al., 2017], such as texture [Geirhos et al., 2019], which do not generalize to novel datasets. At the same time, large distribution shifts between training and test datasets are common in histopathology [Zech et al., 2018, AlBadawy et al., 2018] as a result of tissue preprocessing and image acquisition [Veta et al., 2016, Komura and Ishikawa, 2018, Tellez et al., 2019].

As building robustness against these shifts into models is difficult, they need to "*know when they don't know*" [Shafaei et al., 2018, Roy et al., 2022], i.e., to estimate the uncertainty of their predictions. We review relevant use cases and how methods for uncertainty estimation have been applied in computational histopathology to date.

<sup>1</sup><https://www.fda.gov/news-events/press-announcements/fda-authorizes-software-can-help-identify-prostate-cancer>

## 1.1 Related work

There are (at least) two scenarios where a model has a high predictive uncertainty: when it encounters an unknown sample (out-of-distribution, OOD) or a known (in-distribution, ID) but ambiguous sample. In either case, the model accuracy is likely low and samples should be deferred to a human expert to avoid erroneous predictions. By setting an upper threshold on the uncertainty of samples, uncertainty estimation methods can be used for selective prediction.

**Uncertainty estimation methods** The maximum softmax probability (MSP) [Hendrycks and Gimpel, 2016] is a common baseline estimate of predictive uncertainty, but in general not well calibrated [Guo et al., 2017]. Bayesian neural networks [Mackay, 1992, Buntine and Weigend, 1991, Mackay, 1995] provide a principled approach to quantify model uncertainty but require dedicated architectures, are difficult and expensive to train, hard to scale to large models and datasets, and their uncertainty estimates may not be robust to dataset shift [Ovadia et al., 2019, Gustafsson et al., 2020]. There are various approximations that reduce the computational complexity, such as low rank approximations [Dusenberry et al., 2020] and Markov chain Monte Carlo methods [Welling and Teh, 2011], or that can be transferred to standard network architectures, such as Laplace approximations [MacKay, 1992, Daxberger et al., 2021].

Monte-Carlo (MC) dropout [Gal and Ghahramani, 2016] is a widely used method, as it is easily implemented in architectures with DropOut layers [Hinton et al., 2012]. Currently, state-of-the-art uncertainty estimates are obtained by using the entropy in the predictions of a deep ensemble [Lakshminarayanan et al., 2017], or an efficient approximation thereof [Wen et al., 2020]. Similarly competitive are a number of recently proposed methods that require only a single-forward pass and are "distance-aware" [Tagasovska and Lopez-Paz, 2019, Liu et al., 2020, Mukhoti et al., 2021, Van Amersfoort et al., 2020, Jain et al., 2021]. They use feature space distances between training and test samples to quantify uncertainty. This allows them to accurately estimate uncertainty far away from the decision boundary.

**Uncertainty estimation and OOD detection in histopathology** Several studies in histopathology use deep ensembles [Lakshminarayanan et al., 2017, Pocevičiūtė et al., 2021, Thagaard et al., 2020], while Senousy et al. [2021b] use MSP to select models for an ensemble. Linmans et al. [2020] use an ensembling approach on multiple prediction heads for open set recognition (OSR). Rączkowski et al. [2019] show that MC Dropout-based uncertainty is high for ambiguous or mislabelled patches, but did not test on OOD data; Syrykh et al. [2020] use MC Dropout for both OSR and OOD detection but do not report OOD detection metrics. Note that, MC Dropout can be problematic in network architectures commonly used in computational histopathology<sup>2</sup>, and has been shown to negatively affect task performance [Linmans et al., 2020].

Unfortunately, the OOD detection reported in Syrykh et al. [2020], Pocevičiūtė et al. [2021], Senousy et al. [2021a] is of limited insight, as uncertainty thresholds for selective prediction were set on the same OOD data on which performance was evaluated. Dolezal et al. [2022] avoid such data leakage by setting the uncertainty threshold on validation data using cross-validation. However, it is unclear whether a threshold chosen to distinguish between correct and incorrect ID samples is suitable to separate ID and OOD data. For example, on a dataset for which there is no correct diagnosis, still more than 20% of slides are rated high-confidence by the uncertainty-aware classifier of Dolezal et al. [2022].

## 1.2 Contributions

The uncertainty estimation methods used by previous work like MC Dropout or deep ensembles don't show state-of-the-art performance on standard ML datasets or require substantial additional compute, respectively. They also estimate uncertainty around the decision boundary, i.e. are most suitable to detect ambiguous samples, but may give high confidence estimates for OOD samples far away from the decision boundary. Recently proposed "distance-aware" uncertainty estimation

---

<sup>2</sup> Li et al. [2019] demonstrated that applying MC Dropout with dropout rates  $\geq 0.1$  in networks that use Layer Normalization [Ba et al., 2016] – as is the case in the related work cited above – can be problematic: the combination causes unstable numerical behavior during inference on a range of architectures (DenseNet, ResNet, ResNeXt [Xie et al., 2017] and Wide ResNet [Zagoruyko and Komodakis, 2016]), and requires additional implementation strategies

methods [Tagasovska and Lopez-Paz, 2019, Liu et al., 2020, Mukhoti et al., 2021, Van Amersfoort et al., 2020] address these concerns and present an attractive alternative for histopathology. To the best of our knowledge they have not yet been evaluated on challenging clinical datasets. Because of its superior performance and relative ease of implementation in combination with existing architectures, we chose a spectral-normalized Gaussian Process (SNGP) [Liu et al., 2020] as a representative distance-aware method and compare its performance to methods currently widely used in histopathology.

Our paper makes the following contributions:

- We evaluate the predictive performance and calibration of a baseline (MSP), two commonly used (MC Dropout and deep ensembles), and one distance-aware uncertainty estimation method (SNGP) on CIFAR-10 and compare to two datasets of clinical histopathology data.
- We demonstrate the limitations of using uncertainty thresholding for OOD detection in histopathology; we discuss caveats and areas for further research in applying uncertainty estimation in histopathology.

## 2 Methods

### 2.1 Datasets

First, we evaluate the uncertainty estimation methods on CIFAR-10, to investigate whether their performance on a standard ML dataset transfers to clinical histopathology data. As CIFAR-10 OOD data, we designed image corruptions that emulate realistic histopathological distribution shifts. Using Pytorch’s ColorJitter transform, we randomly change the brightness, contrast, saturation and hue based on ranges we observed in clinical whole-slide images (WSIs) stained with hematoxylin and eosin (H&E) dye (brightness=0, contrast=0, saturation=0.1, hue=0.1).

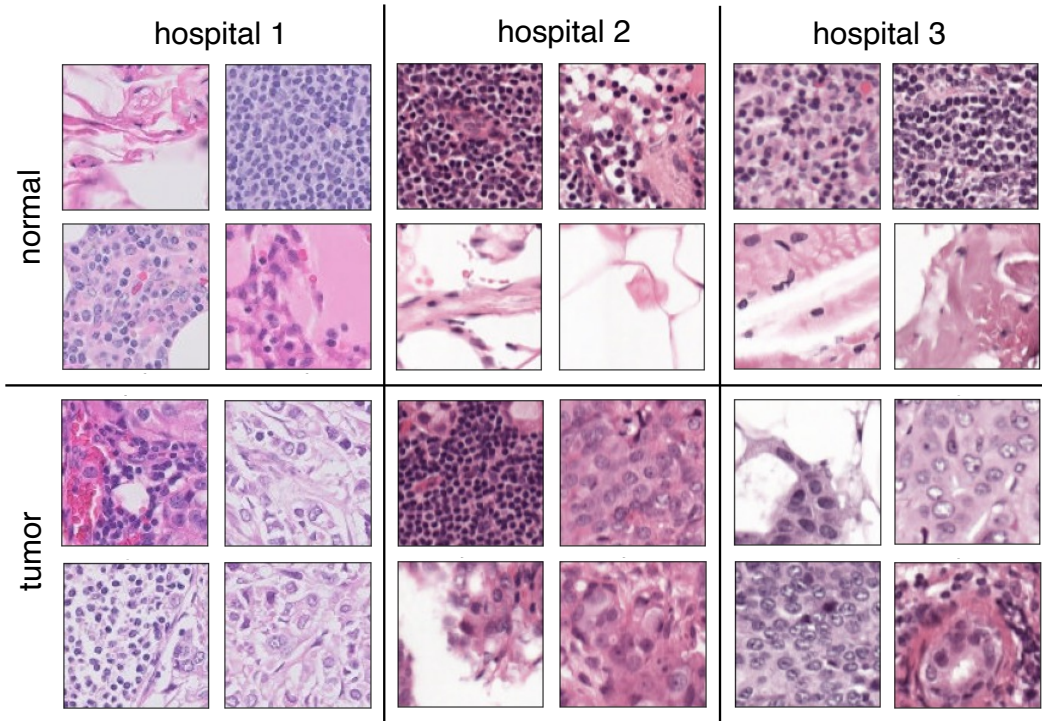


Figure 1: Representative tiles of WSIs from the Camelyon17 dataset, illustrating the variation between normal and tumour tissue, and between different hospitals used as training/validation datasets. While from the same hospitals, training and validation sets are non-overlapping.

Second, we use a patch-based version [Bandi et al., 2018] of the Camelyon17 grand challenge dataset (<https://camelyon17.grand-challenge.org/>), which contains patches of WSIs of

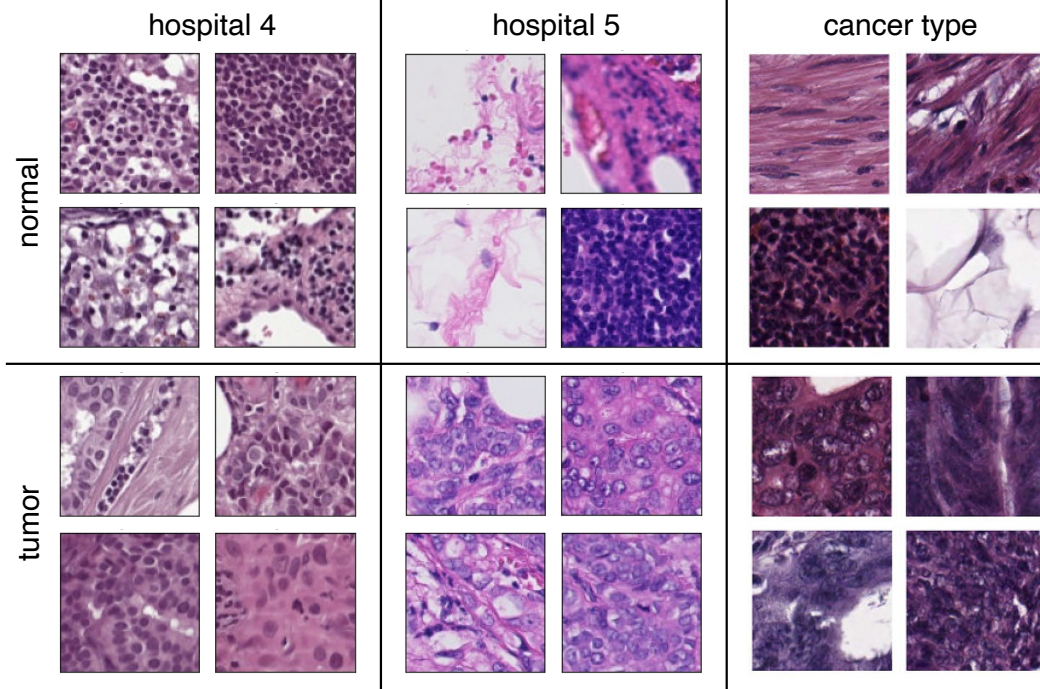


Figure 2: Sample tiles from the Camelyon17 and colorectal cancer dataset [Kather et al., 2016], used as OOD datasets.

H&E stained lymph node sections. This dataset is open source and available under a CC0 1.0 license<sup>3</sup>. Following [Koh et al., 2021], we divide the dataset into four folds according to the hospitals where WSIs were obtained: the training set consists of WSIs taken from three hospitals (hospitals 1–3), each contributing ten WSIs for a total of 302 436 patches. We use three OOD test sets: OOD1 (hospital 4), consisting of 34 904 patches taken from 10 WSIs of a different hospital; OOD2 (hospital 5), consisting of 85 054 patches taken from 10 WSIs of another different hospital<sup>4</sup>. Finally, we evaluate performance to detect a different tumour type on colorectal cancer data from Kather et al. [2016], which is available under a CC BY 4.0 license<sup>5</sup>. For both the Camelyon17 and colorectal cancer datasets the human biological samples were sourced ethically and their research use was in accord with the terms of the informed consents under an IRB/EC approved protocol.

## 2.2 Uncertainty estimation methods

As a baseline we use MSP [Hendrycks and Gimpel, 2016], because it is model-agnostic, and requires no additional implementation effort as it can be read-out from final layer logits. To compare to prior work in histopathology, we use deep ensembles [Lakshminarayanan et al., 2017] and MC Dropout [Gal and Ghahramani, 2016] following implementations in Thagaard et al. [2020] and Kirsch et al. [2019]. For MC Dropout, we add a DropOut layer ( $p=0.5$ , [Hinton et al., 2012]) before the final layer, and perform several forward passes to generate a distribution over predictions (we use 32 MC samples [Ovadia et al., 2019]). We use ensembles with four members. For a brief comparison of uncertainty estimation method characteristics see Table 1.

We also implemented a single forward pass, distance-aware method, SNGP [Liu et al., 2020]. This required modifications to the model architecture: we added a Gaussian Process layer with random feature approximation adapted from <https://github.com/google/edward2>, following Rahimi and Recht [2007]. We also added spectral normalization [Miyato et al., 2018] to the training. For all

<sup>3</sup><https://creativecommons.org/publicdomain/zero/1.0>

<sup>4</sup>Note that in previous work [Koh et al., 2021], OOD1 and OOD2 datasets have been considered "near" and "far" OOD, respectively, based on the more different visual appearance of patches from hospital 5.

<sup>5</sup><https://creativecommons.org/licenses/by/4.0/legalcode>

UE method	model-agnostic	single pass	distance-aware	implementation
Softmax	yes	yes	no	logits
Dropout	yes*	no	no	DropOut Layer; $n$ passes
Ensemble	yes	no	no	$n$ random initializations
SNGP	no	yes	yes	GP Layer; train with SN

Table 1: Comparison of uncertainty estimation methods evaluated. DropOut Layer: <https://pytorch.org/docs/stable/generated/torch.nn.Dropout.html>; GP Layer: <https://github.com/google/edward2>; SN = spectral normalization; \* Potential architectural incompatibilities, see [Li et al., 2019].

models, we train a ResNet-50 [He et al., 2016] for 100 epochs to predict tumor vs normal, using a cross-entropy loss with Adam [Kingma and Ba, 2014] (lr=1e-3, weight decay=1e-5) as an optimizer.

### 2.3 Evaluation metrics

For a dataset of  $N$  input-output pairs  $(x_n, y_n)$ , in our case with a binary label  $y_n$ , we evaluate predictive accuracy, average precision (AP)<sup>6</sup>, Expected Calibration Error (ECE) and Maximum Calibration Error (MCE) [Naeini et al., 2015], which are defined as follows:

$$AP = \sum_{k=1}^K P(k) \Delta r(k) \quad (1)$$

where  $P(k)$  is the precision at threshold  $k$  and  $\Delta r(k)$  is the change in recall from  $k-1$  to  $k$ ,

$$ECE = \sum_{b=1}^B \frac{n_b}{N} |\text{acc}(b) - \text{con}(b)| \quad (2)$$

$$MCE = \max_{b=1, \dots, B} \frac{n_b}{N} |\text{acc}(b) - \text{con}(b)| \quad (3)$$

where  $\text{acc}(b)$  and  $\text{con}(b)$  are the accuracy and confidence of bin  $b$  respectively,  $n_b$  number is the number of predictions in bin  $b$ , and  $B = 15$  is the number of bins.

We also use the AUROC score of distinguishing between ID and OOD data [Lakshminarayanan et al., 2017, Mukhoti et al., 2021]. All of the above metrics are computed on classifier logits. We report results as mean  $\pm$  std, averaged over four random initializations. For ensembles, we report results averaged over three ensembles with four members each, i.e., 12 random initializations in total.

### 2.4 Uncertainty thresholding

To set an uncertainty threshold for selective prediction, we chose Youden’s J statistic [Youden, 1950] because it optimally trades of sensitivity and specificity, and is widely used in diagnostic tests (e.g. [Perkins and Schisterman, 2005]). Youden’s J is defined as follows:

$$J = \frac{TP}{TP + FN} + \frac{TN}{TN + FP} - 1 \quad (4)$$

where TP are true positives, FN are false negatives, TN are true negatives and FP are false positives.

<sup>6</sup>Average precision is less sensitive to class imbalance than accuracy. While our ID validation data, OOD1 and OOD2 datasets are balanced, the colorectal cancer dataset has a 7:1 ratio of normal:tumor tissue.

UE method	Accuracy $\uparrow$	AP $\uparrow$	ECE $\downarrow$	MCE $\downarrow$	AUROC-ood $\uparrow$
validation					
Softmax	0.870 $\pm$ 0.004	0.918 $\pm$ 0.003	0.089 $\pm$ 0.003	0.433 $\pm$ 0.192	-
Dropout	0.868 $\pm$ 0.004	0.919 $\pm$ 0.003	0.089 $\pm$ 0.003	<b>0.319 <math>\pm</math> 0.017</b>	-
Ensemble	<b>0.912 <math>\pm</math> 0.002</b>	<b>0.942 <math>\pm</math> 0.005</b>	<b>0.049 <math>\pm</math> 0.004</b>	<b>0.257 <math>\pm</math> 0.050</b>	-
SNGP	0.854 $\pm$ 0.008	0.906 $\pm$ 0.007	0.104 $\pm$ 0.006	0.451 $\pm$ 0.171	-
OOD					
Softmax	<b>0.490 <math>\pm</math> 0.020</b>	0.618 $\pm$ 0.008	<b>0.370 <math>\pm</math> 0.023</b>	0.520 $\pm$ 0.017	0.785 $\pm$ 0.007
Dropout	0.426 $\pm$ 0.125	0.548 $\pm$ 0.163	0.449 $\pm$ 0.166	0.576 $\pm$ 0.125	0.783 $\pm$ 0.024
Ensemble	<b>0.519 <math>\pm</math> 0.013</b>	<b>0.694 <math>\pm</math> 0.003</b>	<b>0.328 <math>\pm</math> 0.026</b>	0.508 $\pm$ 0.094	<b>0.819 <math>\pm</math> 0.002</b>
SNGP	0.455 $\pm$ 0.024	0.562 $\pm$ 0.020	0.409 $\pm$ 0.032	0.545 $\pm$ 0.033	0.755 $\pm$ 0.015

Table 2: Results on CIFAR-10 validation and CIFAR-10-OOD dataset (= histopathology-like shift), mean  $\pm$  std, averaged over 4 seeds. Highest performing method ( $> 1$  std) in **bold**.

UE method	Accuracy $\uparrow$	AP $\uparrow$	ECE $\downarrow$	MCE $\downarrow$	AUROC-ood $\uparrow$
validation					
Softmax	0.984 $\pm$ 0.015	<b>0.998 <math>\pm</math> 0.003</b>	0.009 $\pm$ 0.010	0.192 $\pm$ 0.038	-
Dropout	0.990 $\pm$ 0.001	0.986 $\pm$ 0.002	0.005 $\pm$ 0.001	0.154 $\pm$ 0.036	-
Ensemble	<b>0.995 <math>\pm</math> 0.000</b>	<b>1.000 <math>\pm</math> 0.000</b>	0.002 $\pm$ 0.000	0.190 $\pm$ 0.056	-
SNGP	0.990 $\pm$ 0.001	0.999 $\pm$ 0.000	<b>0.001 <math>\pm</math> 0.000</b>	<b>0.069 <math>\pm</math> 0.010</b>	-
OOD 1 (hospital 4)					
Softmax	0.765 $\pm$ 0.079	0.793 $\pm$ 0.082	0.211 $\pm$ 0.074	0.335 $\pm$ 0.041	0.623 $\pm$ 0.057
Dropout	<b>0.801 <math>\pm</math> 0.052</b>	0.769 $\pm$ 0.040	0.177 $\pm$ 0.051	0.340 $\pm$ 0.031	0.637 $\pm$ 0.083
Ensemble	<b>0.832 <math>\pm</math> 0.019</b>	<b>0.876 <math>\pm</math> 0.032</b>	0.148 $\pm$ 0.019	0.320 $\pm$ 0.017	0.632 $\pm$ 0.021
SNGP	0.793 $\pm$ 0.065	<b>0.909 <math>\pm</math> 0.031</b>	0.125 $\pm$ 0.063	<b>0.215 <math>\pm</math> 0.075</b>	<b>0.830 <math>\pm</math> 0.042</b>
OOD 2 (hospital 5)					
Softmax	0.624 $\pm$ 0.054	0.662 $\pm$ 0.072	0.325 $\pm$ 0.061	0.363 $\pm$ 0.065	0.765 $\pm$ 0.015
Dropout	<b>0.633 <math>\pm</math> 0.074</b>	0.597 $\pm$ 0.057	0.322 $\pm$ 0.072	0.396 $\pm$ 0.077	0.776 $\pm$ 0.042
Ensemble	0.619 $\pm$ 0.020	0.665 $\pm$ 0.011	0.341 $\pm$ 0.024	0.385 $\pm$ 0.008	0.775 $\pm$ 0.042
SNGP	<b>0.737 <math>\pm</math> 0.038</b>	<b>0.809 <math>\pm</math> 0.045</b>	<b>0.156 <math>\pm</math> 0.032</b>	<b>0.229 <math>\pm</math> 0.031</b>	<b>0.887 <math>\pm</math> 0.032</b>
OOD 3 (cancer type)					
Softmax	0.591 $\pm$ 0.130	0.120 $\pm$ 0.006	0.353 $\pm$ 0.109	0.584 $\pm$ 0.072	0.718 $\pm$ 0.046
Dropout	0.675 $\pm$ 0.102	0.123 $\pm$ 0.002	0.286 $\pm$ 0.085	<b>0.334 <math>\pm</math> 0.064</b>	<b>0.760 <math>\pm</math> 0.081</b>
Ensemble	0.637 $\pm$ 0.021	0.124 $\pm$ 0.000	0.320 $\pm$ 0.013	<b>0.379 <math>\pm</math> 0.033</b>	0.766 $\pm$ 0.031
SNGP	0.631 $\pm$ 0.057	0.124 $\pm$ 0.001	0.304 $\pm$ 0.060	0.432 $\pm$ 0.089	<b>0.851 <math>\pm</math> 0.019</b>

Table 3: Results on Camelyon17 and [Kather et al., 2016] datasets, mean  $\pm$  std averaged over 4 seeds. Highest performing method ( $> 1$  std) in **bold**.

### 3 Experiments

#### 3.1 Predictive performance and calibration

Deep ensembles outperform all other methods both in terms of predictive performance and calibration on both the CIFAR-10 ID and OOD set, however, the drop in performance on OOD data is substantial. The results on CIFAR-10 (Table 2) only somewhat generalize: on histopathology data all methods show strong performance on ID samples, but predictive performance and in particular calibration drops sharply for the far OOD datasets (hospital 5 and cancer type). Different uncertainty estimation methods perform best on different datasets and metrics. Notably, SNGP outperforms all other methods on the hospital 5 OOD dataset.

#### 3.2 OOD detection

All tested UE methods perform poorly on OOD data, in particular the more different the OOD samples are from the training set, even though this "far OOD" detection is considered an easier task than "near OOD" detection [Shafaei et al., 2018]. SNGP has similar performance across the different OOD datasets and consistently outperforms all other methods in OOD detection.



UE method	hospital 4	hospital 5	cancer type
Softmax	$0.658 \pm 0.110$	$0.234 \pm 0.215$	$0.278 \pm 0.208$
Dropout	$0.490 \pm 0.110$	$0.158 \pm 0.133$	$0.211 \pm 0.130$
Ensemble	$0.357 \pm 0.209$	$0.355 \pm 0.237$	$0.344 \pm 0.205$
SNGP	$0.341 \pm 0.114$	$0.169 \pm 0.049$	$0.292 \pm 0.134$

Table 4: Fraction of samples (mean  $\pm$  std) retained after rejection based on an uncertainty threshold that optimizes Youden’s J, set on hospital 5 and hospital 4 for hospital 4 and hospital 5 & cancer type, respectively.

What causes this superior performance? SNGP makes use of feature space distances between training and test samples to quantify uncertainty: it combines a distance-preserving feature extractor, (spectral normalization [Miyato et al., 2018]) with a distance-aware classifier (Gaussian Process [Liu et al., 2020]), i.e., by design it should perform well on distinguishing between OOD and ID data. In addition, our results suggest that the uncertainty estimates of SNGP are also well calibrated on ID data.

### 3.3 Uncertainty thresholding

For selective prediction, we set an uncertainty threshold to separate OOD and ID data. We chose not to set this threshold on ID data; however, setting it on OOD data because it is unclear that this separates well between ID and OOD samples. Instead, we evaluate how well OOD thresholds set on different OOD datasets separate ID from OOD data. In Figure 3 we report results for OOD detection on hospital 4 with threshold set on hospital 5; as well as OOD detection on hospital 5 and a different cancer type, with threshold set on hospital 4. All other combinations can be found in the Appendix. While uncertainty thresholding does in general increase accuracy, the gains are very variable across datasets and methods. Notably a large proportion of samples are rejected across all methods and thresholds (see Table 4), putting into question the practicality of using uncertainty thresholding in clinical practice.

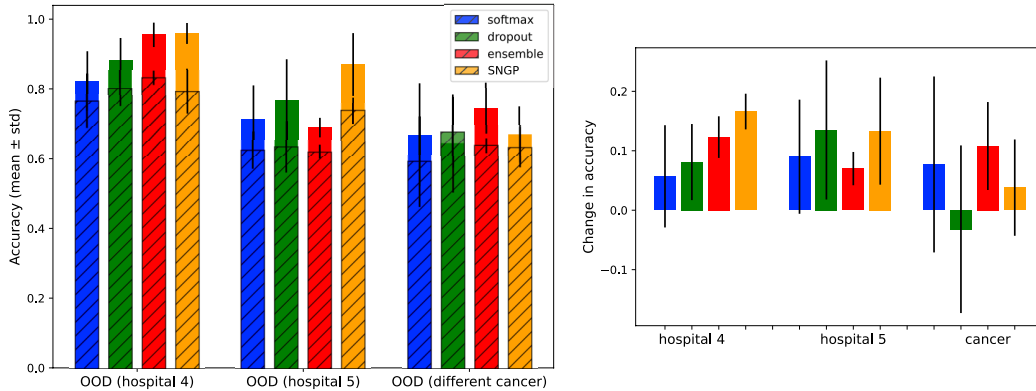


Figure 3: Left: accuracy before (hashed) and after (unhashed bars) uncertainty thresholding. Right: change in accuracy due to thresholding. For results on average precision, see Appendix.

## 4 Discussion

### 4.1 CIFAR-10 vs Camelyon-17/colorectal cancer datasets

We found that the performance of uncertainty estimation methods observed on CIFAR-10 does not generalize well to histopathology datasets. This is in line with previous work demonstrating that several methods which improve model performance and robustness on standard ML datasets have no effect, or decrease model performance, on histopathology data [Tamkin et al., 2022]. Furthermore,

model performance on clinical histopathology datasets exhibits high variance across seeds [Koh et al., 2021], likely also as a result of the highly variable sample collection and processing.

Common ML datasets are very different from clinical histopathology data: first, the CIFAR-10 dataset contains images of a single, centered object, at a low resolution, whereas tiles of histopathology slides often contain many different objects and textures at a high resolution. Second, while there is some noise associated with CIFAR-10 labels [Peterson, Battleday, Griffiths, and Russakovsky, 2019, Wei, Zhu, Cheng, Liu, Niu, and Liu, 2021], the variability of individual pathologists and across pathologists in classifying histopathology images is much larger [Gomes et al., 2014, Tan et al., 2005]. Thus, evaluating models that perform well on standard ML datasets on a range of histopathological data is an important research direction for bringing state-of-the-art ML performance closer to having impact in the clinical practice.

## 4.2 Uncertainty thresholding

While we and others have demonstrated that setting an uncertainty threshold can be used to increase predictive accuracy, both on ID and OOD data, it remains an open problem how to set this crucial hyperparameter: when setting the threshold on ID (validation) data, this may not distinguish well between ID and OOD samples. Conversely, using OOD samples to set this uncertainty threshold *requires access to OOD data*. Not only may OOD data not be available, but a threshold set on one OOD dataset may overfit and not be suitable for samples from another OOD dataset. Furthermore, even in a situation where several sets of OOD data are available, it is unclear whether the uncertainty threshold is best set on OOD data closer or further away (in data and/or feature space) from the ID dataset, or whether and how uncertainty thresholds set on different datasets should be aggregated. While beyond the scope of this paper, these questions form an interesting direction for further research.

## 5 Conclusion

Our work underscores the importance of independent research evaluating state-of-the-art algorithms on challenging datasets beyond the like of CIFAR-10. Based on our work, we expect similar results in other clinical data modalities that share characteristics with histopathology, such as high sample variability, small datasets, and high levels of label noise.

We demonstrate which uncertainty evaluation methods can work well on histopathological data, we caution against relying on individual calibration metrics (see also Appendix). We found that SNGP – a distance-aware method that is sensitive to differences in ID and OOD data – is the best performing uncertainty estimation method on histopathology data. However, we show that the use of uncertainty thresholding for OOD detection or to increase predictive accuracy is problematic in histopathology.

Promising directions for future work will be, first, to test other OOD detection methods, and second, to develop clinically meaningful downstream tasks and datasets on which models and methods can be evaluated. We hope that our work helps to bridge the gap between current developments in ML and histopathology, and encourage developers of novel uncertainty estimation and OOD detection methods to benchmark these not just on standard ML datasets, but also on histopathological data, where their performance is highly relevant for clinical applications.

## Acknowledgements

We thank Stefan Bauer, Robert Vandersluis, Rafael Poyiadzi, Emma Slade and two anonymous reviewers for helpful discussions and comments.



## References

- Ehab A AlBadawy, Ashirbani Saha, and Maciej A Mazurowski. Deep learning for segmentation of brain tumors: Impact of cross-institutional training and testing. *Medical physics*, 45(3):1150–1158, 2018.
- Devansh Arpit, Stanislaw Jastrzebski, Nicolas Ballas, David Krueger, Emmanuel Bengio, Maxinder S. Kanwal, Tegan Maharaj, Asja Fischer, Aaron C. Courville, Yoshua Bengio, and Simon Lacoste-Julien. A closer look at memorization in deep networks. *arXiv preprint*, arXiv:1706.05394, 2017.
- Jimmy Lei Ba, Jamie Ryan Kiros, and Geoffrey E. Hinton. Layer normalization. *arXiv preprint arXiv:1607.06450*, 2016.
- Peter Bandi, Oscar Geessink, Quirine Manson, Marcory Van Dijk, Maschenka Balkenhol, Meyke Hermesen, Babak Ehteshami Bejnordi, Byungjae Lee, Kyunghyun Paeng, Aoxiao Zhong, et al. From detection of individual metastases to classification of lymph node status at the patient level: the camelyon17 challenge. *IEEE Transactions on Medical Imaging*, 2018.
- Wray L. Buntine and Andreas S. Weigend. Bayesian back-propagation. *Complex Syst.*, 5, 1991.
- Erik Daxberger, Agustinus Kristiadi, Alexander Immer, Runa Eschenhagen, Matthias Bauer, and Philipp Hennig. Laplace redux—effortless bayesian deep learning. In *Neural Information Processing Systems*, 2021.
- James M Dolezal, Andrew Srisuwananukorn, Dmitry Karpeyev, Siddhi Ramesh, Sara Kochanny, Brittany Cody, Aaron Mansfield, Sagar Rakshit, Radhika Bansa, Melanie Bois, et al. Uncertainty-informed deep learning models enable high-confidence predictions for digital histopathology. *arXiv preprint arXiv:2204.04516*, 2022.
- Michael Dusenberry, Ghassen Jerfel, Yeming Wen, Yian Ma, Jasper Snoek, Katherine Heller, Balaji Lakshminarayanan, and Dustin Tran. Efficient and scalable Bayesian neural nets with rank-1 factors. In *Proceedings of the 37th International Conference on Machine Learning*, volume 119, pages 2782–2792. PMLR, 13–18 Jul 2020.
- Yarin Gal and Zoubin Ghahramani. Dropout as a bayesian approximation: Representing model uncertainty in deep learning. In *International Conference on Machine Learning*, pages 1050–1059. PMLR, 2016.
- Robert Geirhos, Patricia Rubisch, Claudio Michaelis, Matthias Bethge, Felix Wichmann, and Wieland Brendel. Imagenet-trained cnns are biased towards texture; increasing shape bias improves accuracy and robustness. *arXiv preprint*, arXiv:1811.12231, 2019.
- Douglas Soltau Gomes, Simone Souza Porto, Debora Balabram, and Helenice Gobbi. Inter-observer variability between general pathologists and a specialist in breast pathology in the diagnosis of lobular neoplasia, columnar cell lesions, atypical ductal hyperplasia and ductal carcinoma in situ of the breast. *Diagnostic Pathology*, 9:121 – 121, 2014.
- Chuan Guo, Geoff Pleiss, Yu Sun, and Kilian Q Weinberger. On calibration of modern neural networks. In *International Conference on Machine Learning*, pages 1321–1330. PMLR, 2017.
- Fredrik K Gustafsson, Martin Danelljan, and Thomas B Schon. Evaluating scalable bayesian deep learning methods for robust computer vision. In *Proceedings of the IEEE/CVF conference on computer vision and pattern recognition workshops*, pages 318–319, 2020.
- Kaiming He, Xiangyu Zhang, Shaoqing Ren, and Jian Sun. Deep residual learning for image recognition. In *Proceedings of the IEEE conference on computer vision and pattern recognition*, pages 770–778, 2016.
- Dan Hendrycks and Kevin Gimpel. A baseline for detecting misclassified and out-of-distribution examples in neural networks. *arXiv preprint arXiv:1610.02136*, 2016.
- Geoffrey E Hinton, Nitish Srivastava, Alex Krizhevsky, Ilya Sutskever, and Ruslan R Salakhutdinov. Improving neural networks by preventing co-adaptation of feature detectors. *arXiv preprint arXiv:1207.0580*, 2012.

- Moksh Jain, Salem Lahlou, Hadi Nekoei, Victor Butoi, Paul Bertin, Jarrod Rector-Brooks, Maksym Korablyov, and Yoshua Bengio. Deup: Direct epistemic uncertainty prediction. *arXiv preprint arXiv:2102.08501*, 2021.
- Jakob Nikolas Kather, FG Zöllner, F Bianconi, SM Melchers, LR Schad, T Gaiser, A Marx, and CA Weis. Collection of textures in colorectal cancer histology. *Zenodo* [https://doi.org/10, 5281](https://doi.org/10.5281/2016), 2016.
- Diederik P Kingma and Jimmy Ba. Adam: A method for stochastic optimization. *arXiv preprint arXiv:1412.6980*, 2014.
- Andreas Kirsch, Joost van Amersfoort, and Yarin Gal. Batchbald: Efficient and diverse batch acquisition for deep bayesian active learning. In *Advances in Neural Information Processing Systems*, volume 32, 2019.
- Pang Wei Koh, Shiori Sagawa, Henrik Marklund, Sang Michael Xie, Marvin Zhang, Akshay Balsubramani, Weihua Hu, Michihiro Yasunaga, Richard Lanus Phillips, Irena Gao, Tony Lee, Etienne David, Ian Stavness, Wei Guo, Berton A. Earnshaw, Imran S. Haque, Sara Beery, Jure Leskovec, Anshul Kundaje, Emma Pierson, Sergey Levine, Chelsea Finn, and Percy Liang. Wilds: A benchmark of in-the-wild distribution shifts. In *International Conference on Machine Learning (ICML)*, 2021.
- Daisuke Komura and Shumpei Ishikawa. Machine learning methods for histopathological image analysis. *Computational and structural biotechnology journal*, 16:34–42, 2018.
- Balaji Lakshminarayanan, Alexander Pritzel, and Charles Blundell. Simple and scalable predictive uncertainty estimation using deep ensembles. *Advances in Neural Information Processing Systems*, 30, 2017.
- Xiang Li, Shuo Chen, Xiaolin Hu, and Jian Yang. Understanding the disharmony between dropout and batch normalization by variance shift. In *Proceedings of the IEEE/CVF conference on computer vision and pattern recognition*, pages 2682–2690, 2019.
- Jasper Linmans, Jeroen van der Laak, and Geert J. S. Litjens. Efficient out-of-distribution detection in digital pathology using multi-head convolutional neural networks. In *MIDL*, 2020.
- Jeremiah Liu, Zi Lin, Shreyas Padhy, Dustin Tran, Tania Bedrax Weiss, and Balaji Lakshminarayanan. Simple and principled uncertainty estimation with deterministic deep learning via distance awareness. *Advances in Neural Information Processing Systems*, 33:7498–7512, 2020.
- Yun Liu, Timo Kohlberger, Mohammad Norouzi, George E Dahl, Jenny L Smith, Arash Mohtashamian, Niels Olson, Lily H Peng, Jason D Hipp, and Martin C Stumpe. Artificial intelligence–based breast cancer nodal metastasis detection: Insights into the black box for pathologists. *Archives of pathology & laboratory medicine*, 143(7):859–868, 2019.
- Francesco Locatello, Stefan Bauer, Mario Lucic, Gunnar Raetsch, Sylvain Gelly, Bernhard Schölkopf, and Olivier Bachem. Challenging common assumptions in the unsupervised learning of disentangled representations. In *international conference on machine learning*, pages 4114–4124. PMLR, 2019.
- David J. C. Mackay. A practical bayesian framework for backpropagation networks. *Neural Computation*, 4:448–472, 1992.
- David J. C. Mackay. Probable networks and plausible predictions - a review of practical bayesian methods for supervised neural networks. *Network: Computation In Neural Systems*, 6:469–505, 1995.
- David JC MacKay. Bayesian interpolation. *Neural computation*, 4(3):415–447, 1992.
- Takeru Miyato, Toshiki Kataoka, Masanori Koyama, and Yuichi Yoshida. Spectral normalization for generative adversarial networks. *arXiv preprint arXiv:1802.05957*, 2018.

- Pooya Mobadersany, Safoora Yousefi, Mohamed Amgad, David A Gutman, Jill S Barnholtz-Sloan, José E Velázquez Vega, Daniel J Brat, and Lee AD Cooper. Predicting cancer outcomes from histology and genomics using convolutional networks. *Proceedings of the National Academy of Sciences*, 115(13):E2970–E2979, 2018.
- Jishnu Mukhoti, Andreas Kirsch, Joost van Amersfoort, Philip HS Torr, and Yarin Gal. Deterministic neural networks with appropriate inductive biases capture epistemic and aleatoric uncertainty. *arXiv preprint arXiv:2102.11582*, 2021.
- Mahdi Pakdaman Naeini, Gregory Cooper, and Milos Hauskrecht. Obtaining well calibrated probabilities using bayesian binning. In *Twenty-Ninth AAAI Conference on Artificial Intelligence*, 2015.
- Nikhil Naik, Ali Madani, Andre Esteva, Nitish Shirish Keskar, Michael F Press, Daniel Ruderman, David B Agus, and Richard Socher. Deep learning-enabled breast cancer hormonal receptor status determination from base-level h&e stains. *Nature communications*, 11(1):1–8, 2020.
- Yaniv Ovadia, Emily Fertig, J. Ren, Zachary Nado, D. Sculley, Sebastian Nowozin, Joshua V. Dillon, Balaji Lakshminarayanan, and Jasper Snoek. Can you trust your model’s uncertainty? evaluating predictive uncertainty under dataset shift. *arXiv preprint*, arXiv:1906.02530, 2019.
- Neil J Perkins and Enrique F Schisterman. The youden index and the optimal cut-point corrected for measurement error. *Biometrical Journal: Journal of Mathematical Methods in Biosciences*, 47(4):428–441, 2005.
- Joshua C Peterson, Ruairidh M Battleday, Thomas L Griffiths, and Olga Russakovsky. Human uncertainty makes classification more robust. In *Proceedings of the IEEE/CVF International Conference on Computer Vision*, pages 9617–9626, 2019.
- Milda Pocevičiūtė, Gabriel Eilertsen, Sofia Jarkman, and Claes Lundström. Can uncertainty boost the reliability of ai-based diagnostic methods in digital pathology? *arXiv preprint arXiv:2112.09693*, 2021.
- Łukasz Rączkowski, Marcin Możejko, Joanna Zambonelli, and Ewa Szczurek. Ara: accurate, reliable and active histopathological image classification framework with bayesian deep learning. *Scientific reports*, 9(1):1–12, 2019.
- Ali Rahimi and Benjamin Recht. Random features for large-scale kernel machines. In *Advances in Neural Information Processing Systems*, volume 20. Curran Associates, Inc., 2007.
- Abhijit Guha Roy, Jie Ren, Shekoofeh Azizi, Aaron Loh, Vivek Natarajan, Basil Mustafa, Nick Pawlowski, Jan Freyberg, Yuan Liu, Zach Beaver, et al. Does your dermatology classifier know what it doesn’t know? detecting the long-tail of unseen conditions. *Medical Image Analysis*, 75: 102274, 2022.
- Zakaria Senousy, Mohammed Abdelsamea, Mohamed Medhat Gaber, Moloud Abdar, Rajendra U Acharya, Abbas Khosravi, and Saeid Nahavandi. Mcua: Multi-level context and uncertainty aware dynamic deep ensemble for breast cancer histology image classification. *IEEE Transactions on Biomedical Engineering*, 2021a.
- Zakaria Senousy, Mohammed M Abdelsamea, Mona Mostafa Mohamed, and Mohamed Medhat Gaber. 3e-net: entropy-based elastic ensemble of deep convolutional neural networks for grading of invasive breast carcinoma histopathological microscopic images. *Entropy*, 23(5):620, 2021b.
- Alireza Shafaei, Mark Schmidt, and James J Little. A less biased evaluation of out-of-distribution sample detectors. *arXiv preprint arXiv:1809.04729*, 2018.
- David F Steiner, Po-Hsuan Cameron Chen, and Craig H Mermel. Closing the translation gap: Ai applications in digital pathology. *Biochimica et Biophysica Acta (BBA)-Reviews on Cancer*, 1875(1):188452, 2021.
- Charlotte Syrykh, Arnaud Abreu, Nadia Amara, Aurore Siegfried, Véronique Maisongrosse, François X Frenois, Laurent Martin, Cédric Rossi, Camille Laurent, and Pierre Brousset. Accurate diagnosis of lymphoma on whole-slide histopathology images using deep learning. *NPJ digital medicine*, 3(1):1–8, 2020.

- Natasa Tagasovska and David Lopez-Paz. Single-model uncertainties for deep learning. *Advances in Neural Information Processing Systems*, 32, 2019.
- Alex Tamkin, Dat Nguyen, Salil Deshpande, Jesse Mu, and Noah D. Goodman. Active learning helps pretrained models learn the intended task. *arXiv preprint*, arXiv:2204.08491, 2022.
- PH Tan, S Ho, BC abd Selvarajan, WM Yap, and A Hanby. Pathological diagnosis of columnar cell lesions of the breast: are there issues of reproducibility? *Journal of Clinical Pathology*, 7(58), 2005.
- David Tellez, Geert Litjens, Péter Bándi, Wouter Bulten, John-Melle Bokhorst, Francesco Ciompi, and Jeroen Van Der Laak. Quantifying the effects of data augmentation and stain color normalization in convolutional neural networks for computational pathology. *Medical image analysis*, 58:101544, 2019.
- Jeppe Thagaard, Søren Hauberg, Bert van der Vegt, Thomas Ebstrup, Johan D Hansen, and Anders B Dahl. Can you trust predictive uncertainty under real dataset shifts in digital pathology? In *International Conference on Medical Image Computing and Computer-Assisted Intervention*, pages 824–833. Springer, 2020.
- Joost Van Amersfoort, Lewis Smith, Yee Whye Teh, and Yarin Gal. Uncertainty estimation using a single deep deterministic neural network. In *Proceedings of the 37th International Conference on Machine Learning*, volume 119, pages 9690–9700. PMLR, 13–18 Jul 2020.
- M Veta, PJ van Diest, M Jiwa, S Al-Janabi, and JPW Pluim. Mitosis counting in breast cancer: Object-level interobserver agreement and comparison to an automatic method. *PLoS ONE*, 8(11), 2016.
- Jiaheng Wei, Zhaowei Zhu, Hao Cheng, Tongliang Liu, Gang Niu, and Yang Liu. Learning with noisy labels revisited: A study using real-world human annotations. *arXiv preprint arXiv:2110.12088*, 2021.
- Max Welling and Yee Whye Teh. Bayesian learning via stochastic gradient langevin dynamics. In *ICML*, 2011.
- Yeming Wen, Dustin Tran, and Jimmy Ba. Batchensemble: An alternative approach to efficient ensemble and lifelong learning. *arXiv preprint*, arXiv:2002.06715, 2020.
- Saining Xie, Ross B. Girshick, Piotr Dollár, Zhuowen Tu, and Kaiming He. Aggregated residual transformations for deep neural networks. *2017 IEEE Conference on Computer Vision and Pattern Recognition (CVPR)*, pages 5987–5995, 2017.
- W. J. Youden. Index for rating diagnostic tests. *Cancer*, 3, 1950.
- Sergey Zagoruyko and Nikos Komodakis. Wide residual networks. *arXiv preprint*, arXiv:1605.07146, 2016.
- John R Zech, Marcus A Badgeley, Manway Liu, Anthony B Costa, Joseph J Titano, and Eric Karl Oermann. Variable generalization performance of a deep learning model to detect pneumonia in chest radiographs: a cross-sectional study. *PLoS medicine*, 15(11):e1002683, 2018.

## 6 Appendix

### 6.1 Selective classification results all thresholds – accuracy

threshold set on →	validation	hospital 4	hospital 5	cancer
Softmax				
validation	$0.984 \pm 0.015$	$1.000 \pm 0.000$	$0.999 \pm 0.001$	$0.999 \pm 0.001$
hospital 4	$0.765 \pm 0.079$	$0.821 \pm 0.087$	$0.822 \pm 0.086$	$0.821 \pm 0.085$
hospital 5	$0.624 \pm 0.054$	$0.714 \pm 0.096$	$0.701 \pm 0.115$	$0.714 \pm 0.095$
cancer	$0.591 \pm 0.130$	$0.668 \pm 0.148$	$0.685 \pm 0.156$	$0.684 \pm 0.134$
Dropout				
validation	$0.990 \pm 0.001$	$1.000 \pm 0.001$	$1.000 \pm 0.000$	$0.999 \pm 0.001$
hospital 4	$0.801 \pm 0.052$	$0.932 \pm 0.050$	$0.882 \pm 0.064$	$0.909 \pm 0.040$
hospital 5	$0.633 \pm 0.074$	$0.768 \pm 0.117$	$0.652 \pm 0.150$	$0.748 \pm 0.118$
cancer	$0.675 \pm 0.102$	$0.643 \pm 0.141^*$	$0.596 \pm 0.121$	$0.613 \pm 0.135$
Ensemble				
validation	$0.995 \pm 0.000$	$1.000 \pm 0.000$	$1.000 \pm 0.000$	$1.000 \pm 0.000$
hospital 4	$0.832 \pm 0.019$	$0.924 \pm 0.039$	$0.955 \pm 0.035$	$0.890 \pm 0.021$
hospital 5	$0.619 \pm 0.020$	$0.689 \pm 0.028$	$0.717 \pm 0.054$	$0.682 \pm 0.038$
cancer	$0.637 \pm 0.021$	$0.745 \pm 0.074$	$0.673 \pm 0.090$	$0.787 \pm 0.007$
SNGP				
validation	$0.990 \pm 0.001$	$1.000 \pm 0.000$	$1.000 \pm 0.000$	$1.000 \pm 0.000$
hospital 4	$0.793 \pm 0.065$	$0.961 \pm 0.033$	$0.959 \pm 0.030$	$0.966 \pm 0.034$
hospital 5	$0.737 \pm 0.038$	$0.870 \pm 0.090$	$0.863 \pm 0.085$	$0.883 \pm 0.098$
cancer	$0.631 \pm 0.057$	$0.669 \pm 0.081$	$0.655 \pm 0.090$	$0.695 \pm 0.071$

Table 5: Accuracy across all datasets (columns) for uncertainty thresholds set on all datasets (rows), mean  $\pm$  std, averaged over 4 seeds. \*averaged over 3 seeds, all samples rejected for 1 seed.

### 6.2 Selective classification results all thresholds – average precision

threshold set on →	validation	hospital 4	hospital 5	cancer
Softmax				
validation	$0.979 \pm 0.015$	$0.999 \pm 0.001$	$0.999 \pm 0.001$	$0.998 \pm 0.001$
hospital 4	$0.736 \pm 0.066$	$0.842 \pm 0.162$	$0.777 \pm 0.124$	$0.812 \pm 0.151$
hospital 5	$0.583 \pm 0.039$	$0.656 \pm 0.086$	$0.619 \pm 0.079$	$0.62 \pm 0.087$
cancer	$0.12 \pm 0.006$	$0.155 \pm 0.052$	$0.136 \pm 0.023$	$0.157 \pm 0.042$
Dropout				
validation	$0.986 \pm 0.002$	$0.999 \pm 0.001$	$0.999 \pm 0.000$	$0.999 \pm 0.001$
hospital 4	$0.769 \pm 0.040$	$0.941 \pm 0.062$	$0.881 \pm 0.092$	$0.914 \pm 0.061$
hospital 5	$0.597 \pm 0.057$	$0.644 \pm 0.221$	$0.610 \pm 0.156$	$0.672 \pm 0.210$
cancer	$0.123 \pm 0.002$	$0.260 \pm 0.107^*$	$0.201 \pm 0.080$	$0.225 \pm 0.106$
Ensemble				
validation	$0.993 \pm 0.000$	$1.000 \pm 0.000$	$1.000 \pm 0.000$	$0.999 \pm 0.000$
hospital 4	$0.790 \pm 0.016$	$0.911 \pm 0.046$	$0.951 \pm 0.041$	$0.866 \pm 0.018$
hospital 5	$0.579 \pm 0.015$	$0.603 \pm 0.038$	$0.642 \pm 0.071$	$0.579 \pm 0.034$
cancer	$0.124 \pm 0.000$	$0.231 \pm 0.089$	$0.310 \pm 0.107$	$0.173 \pm 0.011$
SNGP				
validation	$0.986 \pm 0.002$	$1.000 \pm 0.000$	$1.000 \pm 0.000$	$1.000 \pm 0.000$
hospital 4	$0.765 \pm 0.055$	$0.870 \pm 0.121$	$0.869 \pm 0.110$	$0.881 \pm 0.118$
hospital 5	$0.693 \pm 0.032$	$0.613 \pm 0.300$	$0.633 \pm 0.281$	$0.632 \pm 0.316$
cancer	$0.124 \pm 0.001$	$0.253 \pm 0.063$	$0.262 \pm 0.085$	$0.291 \pm 0.084$

Table 6: Average precision across all datasets (columns) for uncertainty thresholds set on all datasets (rows), mean  $\pm$  std, averaged over 4 seeds. \*averaged over 3 seeds, all samples rejected for 1 seed.

### 6.3 Limitations of uncertainty estimation metrics

While metrics can be indicative of performance, ideally, uncertainty estimation methods should be evaluated in a clinical setting, i.e., whether and by how much the quality of their uncertainty estimates affects diagnosis and therefore improves patient outcomes. This is difficult to implement in histopathology: all ML models intended for use in healthcare, in particular if algorithmic predictions directly affect patients, would have to demonstrate their practical benefits for improving diagnostic accuracy and patient outcomes through rigorous embedding and evaluating the model in a clinical trial<sup>7</sup>. In addition to the logistical [Steiner et al., 2021] and financial requirements, there are currently no established best practices and only minimal, non-technical regulatory frameworks for such a scenario.

As a result, there are currently no histopathology models used in the clinic on which such an analysis could be performed. Furthermore, there is no data, such as survival data, that we could have used as a clinically relevant "downstream" task [Locatello et al., 2019], for the Camelyon17 dataset. Lacking relevant data for a downstream task, we explored whether uncertainty estimates could benefit the classification of a model's learnt features into four different cancer stages<sup>8</sup>. We did not find reliable improvements in classification performance as a consequence of better uncertainty estimates, and the results were inconsistent across uncertainty estimation methods and stages. Thus, while beyond the scope of this paper, developing datasets to evaluate uncertainty estimation methods on clinically meaningful downstream tasks is another promising direction for future work.

---

<sup>7</sup>To date, the U.S. Food and Drug Administration (FDA) has approved only one ML-based software, "*Paige Prostate*". Its use is limited to *assisting* pathologists in their assessment, and the associated clinical study did not evaluate the software's impact on final patient diagnosis.

<sup>8</sup>These were: negative (no metastases); isolated tumour cells (single tumour cells or a cluster of tumour cells, not larger than 0.2mm or less than 200 cells); micro-metastasis (larger than 0.2mm and/or containing more than 200 cells, but not larger than 2mm); and macro-metastasis (larger than 2mm). For more details see [Bandi et al., 2018].